analytical chemistry

pubs.acs.org/ac Article

Sensitive and Robust One-Pot RPA-CRISPR/Cas12a Assay with Elimination of *cis*-Cleavage

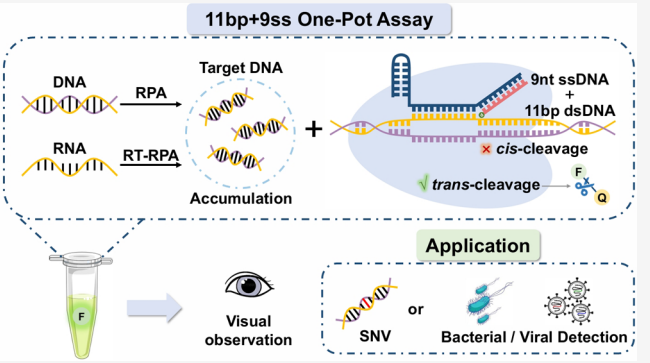
Ruiying Han, Ning Xiao, Zhirui Wu, Yingying Zhao, Xiaoli Wang, and Xiaochuan Tang*

Cite This: https://doi.org/10.1021/acs.analchem.5c06674 Read Online

ACCESS | Metrics & More | Article Recommendations | Supporting Information

Downloaded via SOUTHWEST UNIV on May 3, 2026 at 09:19:05 (UTC).
See https://pubs.acs.org/sharingguidelines for options on how to legitimately share published articles.

ABSTRACT: The rapid detection technology utilizing CRISPR/Cas12a is characterized by high sensitivity, portability, and efficiency, making it a prominent focus in the field of point-of-care testing (POCT). However, it still has limitations in one-pot detection systems. This study developed a one-pot assay based on CRISPR/Cas12a and RPA (11bp+9ss one-pot assay), which nearly eliminates the *cis*-cleavage activity of Cas12a while retaining its *trans*-cleavage activity. Specifically, *cis*-cleavage was abolished by shortening the complementary length between the crRNA and the target to maintain the double-stranded conformation at the *cis*-cleavage site, whereas *trans*-cleavage activity was preserved by using an ssDNA complementary to the remaining region. The *trans*-cleavage activity was applicable to targets within a 200 bp range and under suboptimal PAM conditions. Moreover, rational design of the ssDNA enables effective discrimination of single-base mutations. The 11bp+9ss one-pot assay achieved a limit of detection (LOD) of 1×10^0 copies/μL for various targets, demonstrating robust performance even in suboptimal RPA systems. Furthermore, the assay was successfully applied to the detection of *Salmonella* and Avian Leukosis Virus subgroup J (ALV-J) samples. Overall, the 11bp+9ss one-pot assay exhibits superior sensitivity and robustness, showing great potential for POCT of bacteria and viruses.



INTRODUCTION

Outbreaks of viruses such as SARS-CoV-2 have highlighted the critical need for rapid and efficient monitoring systems to control infectious disease outbreaks.[1−3] Pathogen detection in food, animal, and agricultural products is also crucial for safeguarding public health and economic stability. However, conventional PCR based methods are time-consuming and instrument-dependent, which limits their suitability for rapid response and field testing. Point-of-care testing (POCT) methods, including antigen tests and isothermal amplification techniques—such as recombinase polymerase amplification (RPA)—can deliver rapid results but are hampered by limited sensitivity and high false-negative rates.[4,5] CRISPR technology has emerged as a powerful tool in molecular diagnostics. Cas proteins, with Cas12a as a representative example, specifically recognize and cleave target nucleic acids while exhibiting *trans*-cleavage activity against nonspecific sequences.[6−8] By integrating CRISPR with isothermal amplification, CRISPR-based diagnostics significantly enhance the sensitivity and specificity of pathogen detection, offering a promising approach for rapid and accurate diagnosis.

Conventional CRISPR-based diagnostics have traditionally relied on a two-step process: an initial nucleic acid amplification step followed by CRISPR-mediated detection. This sequential approach is often time-consuming, operationally complex, and increases the risk of aerosol contamination.[9] Integrated one-pot systems, which combine amplification and detection within a single sealed tube, present a promising alternative. A central challenge in developing these systems lies in preventing the *cis*-cleavage activity of Cas12a from interfering with the amplification. Current strategies often depend on the physical or temporal separation of these steps, employing techniques such as microfluidics[9,10] or light-activated crRNAs.[9,11,12] Despite these innovations, challenges related to prolonged detection time, complexity, and cost persist. Recent studies indicate that suppressing Cas12a's *cis*-cleavage activity—by targeting suboptimal PAM sequences or adding inhibitors like heparin—enables simplified one-pot detection.[13−15] This strategy is advantageous due to its operational simplicity and cost-effectiveness. However, a significant limitation is that the detection sensitivity of these systems may be compromised under nonideal amplification conditions. Therefore, a method that completely abolishes *cis*-cleavage while preserving *trans*-cleavage activity would address

Received: October 30, 2025
Revised: April 22, 2026
Accepted: April 24, 2026

© XXXX American Chemical Society

https://doi.org/10.1021/acs.analchem.5c06674
Anal. Chem. XXXX, XXX, XXX−XXX

a fundamental limitation of current one-pot assays, though this goal remains to be achieved.

The cleavage activity of the Cas12a protein is mediated by its RuvC domain. Upon crRNA-guided recognition and unwinding of the target double-stranded DNA (dsDNA), the resulting binding induces a conformational change that activates the RuvC catalytic domain. The activated RuvC domain cleaves the nontarget strand within the region 13−19 distal to the PAM (mainly at position 18) and the target strand within the region 21−24 nucleotides (primarily at position 23), resulting in *cis*-cleavage.[16,17] Once activated, the RuvC domain retains nuclease activity and cleaves single-stranded DNA (ssDNA) nonspecifically, thereby exhibiting *trans*-cleavage activity. Given that the RuvC domain cleaves only ssDNA and that *cis*-cleavage is confined to the 13−24 region due to the spatial constraints between the RuvC domain and the DNA strands, we hypothesize that it may be feasible to activate the RuvC domain while preventing *cis*-cleavage—by maintaining the duplex conformation at the *cis*-cleavage sites—without compromising its *trans*-cleavage activity.

By reducing the complementarity length to preserve the duplex conformation at the *cis*-cleavage sites, we successfully activated the *trans*-cleavage activity of Cas12a with complementary ssDNA while eliminating its *cis*-cleavage activity, which was verified by in vitro cleavage assays. This strategy generated sufficient activity for targets of different lengths and PAM sequences. We subsequently developed a one-pot RPA-CRISPR assay that exhibited a favorable LOD, reliable performance under suboptimal RPA conditions, and successful detection of *Salmonella* and Avian Leukosis Virus subgroup J (ALV-J) in practical samples. Consequently, this study offers valuable insights for building and optimizing effective one-pot detection methods under demanding conditions.

MATERIALS AND METHODS

LbCas12a Protein and Single-Stranded Oligonucleotides (ssDNA)

LbCas12a protein (#32108−03) and the FQ-ssDNA reporter (#31101) were purchased from Tolo Biotech Co., Ltd. (Shanghai, China). Single-stranded oligonucleotides (ssDNA) were synthesized and processed by GENEWIZ (Suzhou, China). The sequences of all ssDNA oligonucleotides used in the various experiments were listed in the Supplementary Tables 1, 5, 8. All ssDNAs of different lengths complementary to the spacer in the one-pot system underwent dideoxycytosine (ddC)-3′ oligo modifications and were purified 2−3 times to ensure that all ssDNAs were modified.

Preparation of Double-Stranded DNA (dsDNA) Targets

The 45 bp dsDNA targets were 90 nt ssDNA containing the PAM and target sequences, synthesized by GENEWIZ (Suzhou, China). The ssDNA were incubated at 95 °C for 5 min and then cooled to 4 °C at a rate of 0.1 °C/s to form a 45 bp double-stranded hairpin structure through annealing. The sequences of the 45 bp dsDNA for each gene were listed in Supplementary Tables 6, 7, 9. Other dsDNA targets of varying lengths were amplified by PCR from pUC-GW plasmids (GENEWIZ, Suzhou, China), which contained multiple chemically synthesized gene sequences and targets. PCR primers were synthesized by GENEWIZ (Suzhou, China), and the primer sequences were provided in Supplementary Table 11. The target DNA bands were separated via electrophoresis on a 1% agarose gel (1× TBE buffer, 300 V, 15 min) and subsequently purified using an Agarose Gel DNA Recovery Kit (Omega Biotek, Georgia, USA).

Preparation of crRNA

The crRNA targeting the pseudorabies virus (PRV) *gE46* gene was obtained through in vitro transcription. A sequence containing the T7 promoter, spacer, and scaffold was designed and synthesized as two complementary single-stranded oligonucleotides (Supplementary Table 2). The two oligonucleotides were incubated at 95 °C for 5 min and then cooled to 4 °C at a rate of 0.1 °C/s to allow annealing, forming double-stranded DNA. The resulting product was separated by 2% agarose gel electrophoresis, and the DNA fragment was purified using a DNA purification kit (Jianshi Biotech, Zhejiang, China) to serve as the template for in vitro transcription. According to the manufacturer's protocol, crRNA was generated by incubating the DNA template at 37 °C for 6 h using an in vitro transcription kit (Thermo Fisher Scientific, Waltham, MA, USA). The DNA template was subsequently digested with DNase I (Vazyme, Nanjing, China) at 37 °C, and the crRNA was purified by the phenol-chloroform method. The crRNAs for other targets in this study were synthesized by GenScript Biotech Corporation (Nanjing, China). The sequences of the crRNAs and their corresponding target sequences were listed in Supplementary Tables 3, 4. Prior to subsequent experiments, ssDNA and crRNA of various lengths prepared in Section were coincubated at 95 °C for 5 min, followed by annealing to 4 °C at a cooling rate of 0.1 °C/s. The ssDNA−crRNA hybrids were stored at − 20 °C for long-term preservation and thawed immediately before use in the one-pot assay.

Detection of *cis*-Cleavage Activities

The *cis*-cleavage activity was verified through in vitro cleavage assays by mixing LbCas12a protein with crRNAs specific to each gene. All reagents were kept on ice. A reaction mixture containing 3 pmol LbCas12a, 7.5 pmol crRNA, 7.5 pmol ssDNA, 2 μL of 10× HOLMES Buffer (Tolo Biotech, Shanghai, China), and 1 pmol Target DNA was prepared, and DEPC-treated water (Thermo) was added to bring the total volume to 15 μL. The mixture was incubated at 37 °C for 1 h. The in vitro cleavage results were analyzed by 1% agarose gel electrophoresis and visualized using a fully automated gel imaging system (Bio-Rad, Berkeley, California, USA).

One-Pot Assay

RPA (Cat# WLB8201KIT) and RT-RPA (Cat# WLRB8207KIT) kits were purchased from Amp-Future Biotech Co., Ltd. (Changzhou, China). A premix was prepared by adding 30 μL of Buffer A, 2 μL each of 20 μM RPA forward primer and 20 μM RPA reverse primer, and 14 μL of DEPC-treated water into a lyophilized reaction tube. The RPA primers were listed in Supplementary Table 10. Then, 9 μL of this premix was supplemented with the following components: 7.5 pmol of ssDNA, 7.5 pmol of crRNA (both ssDNA and crRNA were pretreated as described in Section), 3 pmol of LbCas12a, 2 μL of Buffer B, 1 pmol of FQ-ssDNA reporter, and 1 pmol of DNA target. In experiments investigating the effects of environmental contaminants on the one-pot assay, 2 μL of hemin (derived from plasma samples),[18] 2 μL of ethanol (EtOH, from nucleic acid extracts),[19] and 200 ng of humic acid (from soil or farm litter-contaminated fecal samples)[20] were separately spiked into each reaction group. Fluorescence signals were recorded every 5 s at 37 °C using a real-time PCR system (Roche LightCycler 480 II). The assay was also monitored under blue light (Bio-Rad, Berkeley, California, USA). For quantification of DNA targets, real-time fluorescence curves were analyzed, and the point of inflection (POI) time was calculated according to the following equation:

$$\frac{d^2F}{dt^2} = 0$$

where F denotes fluorescence intensity at a given time and t represents the corresponding time. Subsequently, a standard curve between POI time and DNA concentration was established via linear regression to determine the coefficient of determination (R^2). An $R^2 > 0.9$ was considered acceptable for reliable quantification.[21]

Preparation of Bacterial and Viral Samples

Salmonella and ALV-J strains, as well as other bacterial strains for specificity testing, were kindly provided by the Guangxi Veterinary Research Institute. Practical samples of *Salmonella* were collected from the surfaces of freshly laid eggs. The surface of each egg was

https://doi.org/10.1021/acs.analchem.5c06674
Anal. Chem. XXXX, XXX, XXX−XXX

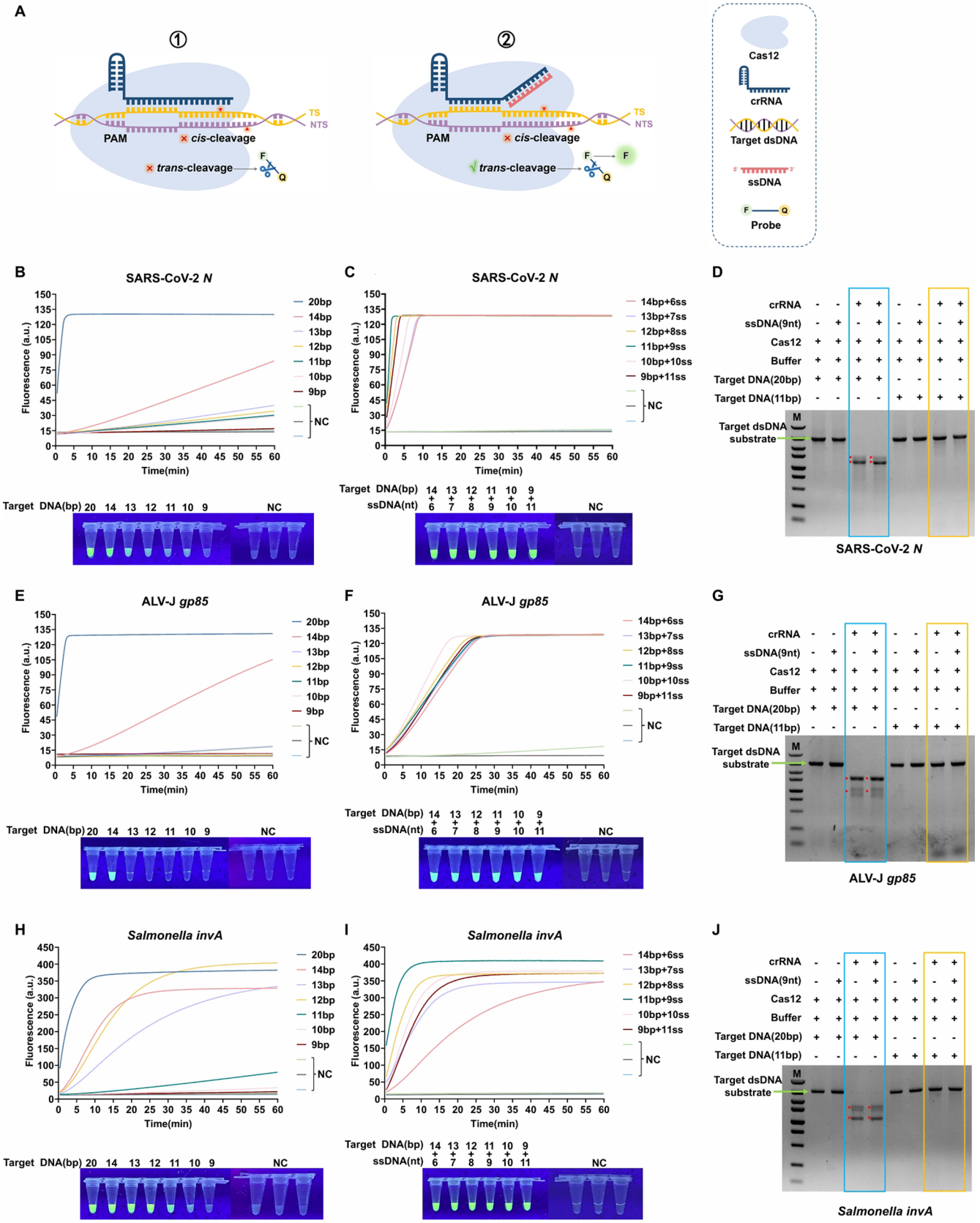


Figure 1. dsDNA and ssDNA of different lengths on the *cis*- and *trans*- cleavage activities of LbCas12a. (A) Schematic diagram showing the *cis*- and *trans*-cleavage activities of LbCas12a by target dsDNA and target ssDNA. TS indicates the target strand, and NTS indicates the nontarget strand. (B, E, H) Designing 45 bp hairpins with target sequences of varying lengths for crRNAs against SARS-CoV-2 *N*, ALV-J *gp85*, and *Salmonella invA*, to evaluate the *trans*-cleavage activity and the direct observation under blue light. (C, F, I) The design of crRNA targeting SARS-CoV-2 *N*, ALV-J *gp85*, and *Salmonella invA* includes 45 bp hairpins carrying target dsDNA of different lengths, as well as ssDNA, to assess their *trans*-cleavage

https://doi.org/10.1021/acs.analchem.5c06674
Anal. Chem. XXXX, XXX, XXX−XXX

Figure 1. continued

activity and the results of direct observation under blue light. (D, G, J) The *trans*-cleavage activity using 11 bp dsDNA and 9 nt ssDNA (hereinafter referred to as 11bp+9ss) was applied to SARS-CoV-2 *N*, ALV-J *gp85*, and *Salmonella invA*. The crRNA used was fully complementary to the 20 bp DNA. The *cis*-cleavage activity of the 11bp+9ss strategy was validated through in vitro cleavage. Green arrows indicate DNA substrates approximately 3000 bp in length carrying 20 bp or 11 bp target sequences, red arrows indicate the cleaved fragments, and M denotes the 5000 bp marker. NC represents three negative controls without DNA substrate, crRNA, or LbCas12a, respectively.

carefully swabbed using a cotton swab moistened with sterile Buffered Peptone Water (BPW). The swab tip containing the bacterial sample was placed in 50 μL of Lysis Buffer (TAKARA) and heat-denatured at 80 °C for 15 min. After centrifugation, the supernatant was collected for subsequent detection. ALV-J samples were collected from chick meconium. The peri-anal area of chicks was swabbed with a BPW-moistened cotton swab. Viral RNA was extracted using an RNA/DNA Extraction Kit (TAKARA) and stored at −80 °C.

qPCR and RT-qPCR Assays

Based on the published *Salmonella* and ALV-J sequences in GenBank, specific primers were designed using Primer (primer sequences were listed in the Supplementary Table 12). For the qPCR assays detecting *Salmonella* samples, a 10 μL reaction system was prepared containing 5 μL of 2× Taq Pro Universal SYBR qPCR Master Mix (Vazyme), 5 μM each of the forward and reverse primers, and 1 μL of the sample. DEPC-treated water was added to bring the total volume to 10 μL. For the RT-qPCR assays detecting ALV-J samples, a 10 μL reaction system was prepared containing 5 μL of 2× one-step SYBR Green mix, 5 μM each of the forward and reverse primers, and 1 μL of the sample. DEPC-treated water was added to a final volume of 10 μL. The volume of sample added for detection and the sample processing method were kept consistent across the qPCR, RT-qPCR, and one-pot assays. A real-time PCR instrument (Roche LightCycler 480 II) was used to determine the cycle threshold (C_t) values for each positive sample, a sample was considered positive if its C_t < 30.

Data Visualization and Statistics

Conventional primers were designed using Primer 5.0 software. Graphs were generated using GraphPad Prism 9.0.0 software. Conduct a conservation analysis of the ALV-J target using DNAMAN 9.0. Each experiment was performed in triplicate, and one representative result was shown. Data supporting the findings of this study are available within the article and its Supporting Information.

RESULTS

Effects of dsDNA and Spacer-Complementary ssDNA on the *trans*- and *cis*-Cleavage Activities of LbCas12a

To maintain the double-stranded state of the PAM-distal dsDNA, we reduced the length of the spacer sequence in the crRNA that is complementary to the dsDNA and assessed the *trans*-cleavage activity of LbCas12a (Figure 1A). We designed and synthesized the crRNAs targeting the SARS-CoV-2 nucleocapsid gene (SARS-CoV-2 *N*), ALV-J *gp85*, *Salmonella invA*, pseudorabies virus (PRV) *gE46*, and *E. colirfbE* for verification. The results demonstrated that for the *Salmonellai nvA*, PRV *gE46*, and *E. colirfbE*, the observed *trans*-cleavage activity was significantly attenuated when the length of the dsDNA complementary to the spacer was less than 11 bp (Figure 1H and Figure S1A,D). For SARS-CoV-2 *N* and ALV-J *gp85*, the *trans*-cleavage activity could not be effectively activated when the length of the complementary dsDNA was less than 14 bp (Figure 1B,E). To maximize the activation of Cas12a *trans*-cleavage activity, supplementation with an ssDNA complementary to the remaining region of the crRNA spacer enabled the *trans*-cleavage activity for each target gene to reach peak levels within 30 min (Figure 1C,F,I and Figure S1B,E). In contrast, the addition of ssDNA alone failed to activate *trans*-cleavage (Figure S2A−F). These results demonstrated that LbCas12a can still activate *trans*-cleavage activity in the presence of minimally paired dsDNA when provided with an additional ssDNA.

Based on a comprehensive evaluation of fluorescence activation intensity, ssDNA-crRNA binding affinity, and distance from the *cis*-cleavage site, a system consisting of 11 bp of dsDNA complementary to the spacer and a 9 nt ssDNA (designated as 11bp+9ss group) was selected for subsequent experiments. The *cis*-cleavage activity of LbCas12a was examined using an in vitro cleavage assay. The results revealed that, in contrast to the positive control with a fully matched 20 bp target site (20 bp group), no cleaved bands were detectable for any of the target genes in the 11bp+9ss group (Figure 1D,G,J, and Figure S1C,F), indicating an absence of *cis*-cleavage activity. In summary, by employing a shortened dsDNA complementary to the spacer in combination with a ssDNA, we successfully activated *trans*-cleavage activity without inducing detectable *cis*-cleavage activity.

Characterization of the *trans*-Cleavage Efficiency of the 11bp+9ss Strategy

Due to the absence of *cis*-cleavage activity, the retained distal region of the dsDNA may affect the accessibility of the probe to the LbCas12a catalytic domain. The *trans*-cleavage activity was assessed using four dsDNA substrates of different lengths (ranging from 45 to 3000 bp) targeting the SARS-CoV-2 *N*, ALV-J *gp85*, and *Salmonella invA*. The results revealed that the targets SARS-CoV-2 *N* and *Salmonella invA* in the 11bp+9ss group exhibited a distinct dsDNA length-dependent *trans*-cleavage activity (Figure S3A,C). In contrast, the 20 bp group showed almost no effect from dsDNA length (Figure S4A,C). For ALV-J *gp85*, the activity remained unaffected within the 45−800 bp range, with a reduction observed only at 3000 bp, both in the 11bp+9ss group (Figure S3B) and the 20 bp group (Figure S4B). These results indicate that dsDNA length does influence the *trans*-cleavage efficiency of the 11bp+9ss system for some targets. Nevertheless, the 11bp+9ss system retained sufficient activity for substrates shorter than 200 bp, which falls within the optimal amplicon size range for RPA amplification.

The number of available PAMs determines the versatility of CRISPR applications. Spacers utilizing VTTV, TTVV, and TCTV PAMs theoretically increase the number of available PAMs by approximately 7-fold compared to the canonical TTTV PAM.[13] Based on this, we evaluated the impact of these suboptimal PAMs on *trans*-cleavage activity using the 11bp +9ss group for the SARS-CoV-2 *N*, ALV-J *gp85*, and *Salmonella invA*. The results showed that the *trans*-cleavage activity for each gene remained consistent across different PAMs (Figure S3D−F), which aligned with the results from the 20 bp group (Figure S4D−F). This indicates that the 11bp +9ss strategy is not constrained by the canonical PAM requirement.

https://doi.org/10.1021/acs.analchem.5c06674
Anal. Chem. XXXX, XXX, XXX−XXX

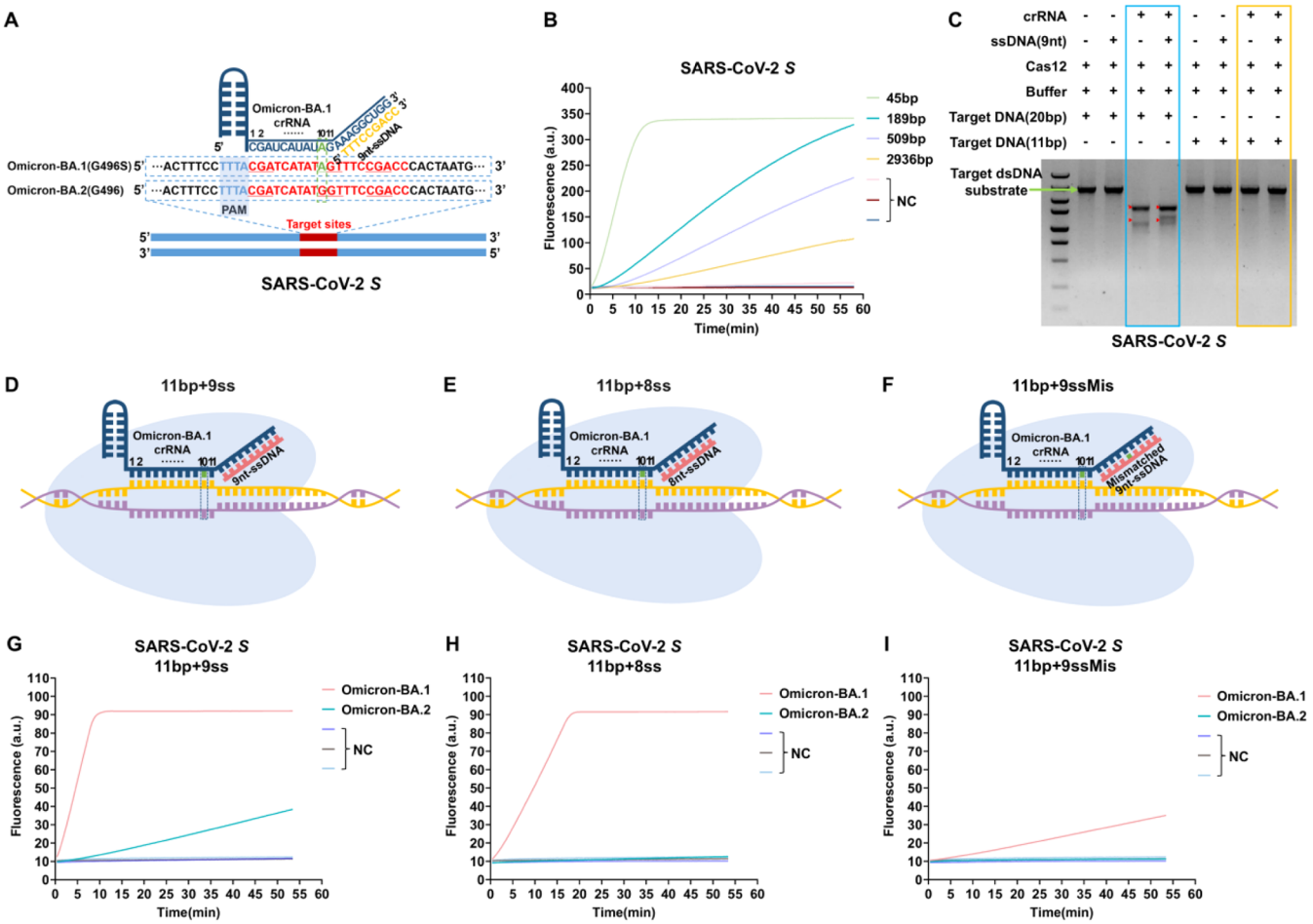


Figure 2. SNV discrimination after optimizing the ssDNA in the 11bp+9ss strategy. (A) Design crRNA targeting the SNV present on the SARS-CoV-2 variant BA.1, aligning the 10th position of the spacer with the SNV, and use the 11bp+9ss strategy to differentiate between the SARS-CoV-2 Omicron BA.1 (G496S) and Omicron BA.2 (G496) strains. (B) Four DNA substrates ranging from 45 to 3000 bp in length, in order to assess the *trans*-cleavage activity of the 11bp+9ss strategy. (C) *Cis*-cleavage activity was assessed through an in vitro cleavage assay. The green arrows indicate DNA substrates approximately 3000 bp in total length, carrying either a 20 bp or 11 bp target sequence, while the red arrows represent the cleaved fragments. M denotes the 5000 bp marker. (D−F) Schematic diagram illustrating the identification of naturally occurring SNVs in the SARS-CoV-2 Omicron BA.1 strain using different approaches. (D) The conventional 11bp+9ss strategy proposed in the study. (E) The 9 nt ssDNA was shortened by 1 nt, represented as 11bp+8ss. (F) 1 nt mismatch was designed in the center of the 9 nt ssDNA, with the green square indicating the position of the mismatched base, represented as 11bp+9ss Mis. (G−I) SNV sites were identified using the three schemes in D−F. NC represents negative controls without DNA substrate, crRNA, or LbCas12a, respectively.

RNA viruses, such as SARS-CoV-2, continuously acquire single-nucleotide variants (SNVs) during transmission, leading to the emergence of new subtypes with altered virulence and infectivity.[22,23] CRISPR-based diagnostics with single-nucleotide resolution are therefore crucial for accurately identifying different viral subtypes. Studies have shown that split substrate can improve the discrimination of SNVs.[24] To validate this, we introduced five SNVs (MT1, 2, 6, 10, 11) at two target sites within the SARS-CoV-2 *N* gene and detected them using the 11bp+9ss strategy (Figure S5A). The results indicated that each SNV only slightly delayed the generation of the fluorescence signal (Figure S5D,G), demonstrating that the 11bp+9ss system lacks practical utility for distinguishing SNVs. Given the flexibility in the length and pairing design of ssDNA, we shortened the ssDNA length (11bp+8ss) or introduced a single mismatch (11bp+9ssMis) (Figure S5B,C). The results showed that both the 11bp+8ss and 11bp+9ssMis enabled rapid detection of the SARS-CoV-2 *N* wild-type (WT) while producing nearly no fluorescence signal for MT10 and only a weak signal for MT11 (Figure S5E,F). Although the 11bp+8ss and 11bp+9ssMis designs could not differentiate SNVs in the suboptimal SARS-CoV-2 *N* target (Figure S5H,I), further optimization by combining both shortening and mismatch strategies (11bp+8ssMis) (Figure S5J) allowed strong fluorescence signals for the WT while yielding nearly no signal for MT10 and MT11 (Figure S5K). These findings demonstrate that rational design of the ssDNA can achieve single-nucleotide resolution, with the diagnostic window located MT10 and MT11.

Omicron BA.1, a SARS-CoV-2 variant that once served as a predominant circulating strain, exhibits enhanced transmissibility, we designed a crRNA targeting a subtype-specific mutation site (G496S, Figure 2A) in the Omicron BA.1 *S* gene,[25,26] and the results showed that this crRNA, when used with the 11bp+9ss system, exhibited sufficient *trans*-cleavage activity against substrates of different lengths (Figure 2B), while no *cis*-cleavage activity was observed (Figure 2C). We further evaluated the detection performance of the 11bp+9ss, 11bp+8ss, and 11bp+9ssMis systems for the G496S mutation. The results demonstrated that the 11bp+8ss system retained

https://doi.org/10.1021/acs.analchem.5c06674
Anal. Chem. XXXX, XXX, XXX−XXX

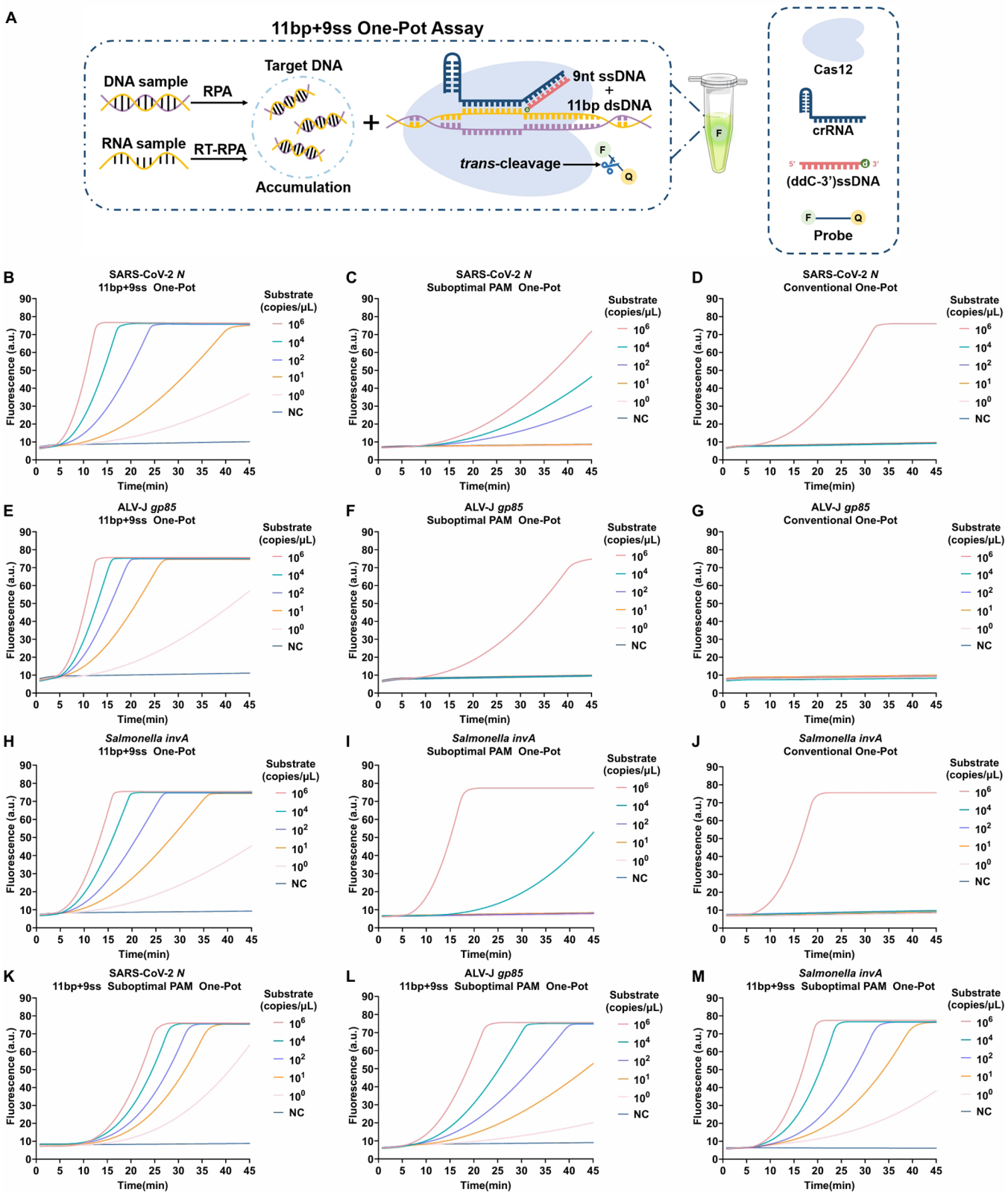


Figure 3. 11bp+9ss one-pot assay. (A) Schematic diagram of the 11bp+9ss one-pot assay. In the one-pot assay, ssDNA was modified with dideoxycytosine (ddC). (B, E, H) Based on the 11bp+9ss strategy, crRNAs targeting conventional target sites were used in combination with RPA to establish a one-pot method for characterizing the plasmid LOD of SARS-CoV-2 *N*, ALV-J *gp85*, and *Salmonella invA*. (C, F, I) Based on the conventional (20bp) scheme, using crRNAs targeting suboptimal target sites, combined with RPA to establish a one-pot method, we characterized the plasmid LOD for detecting SARS-CoV-2 *N*, ALV-J *gp85*, and *Salmonella invA*. (D, G, J) Based on the conventional (20 bp) scheme, using crRNAs targeting conventional target sites, a one-pot method was established in combination with RPA to characterize the plasmid LOD for SARS-CoV-2 *N*, ALV-J *gp85*, and *Salmonella invA*. (K, L, M) Based on the 11bp+9ss strategy, using crRNA targeting suboptimal sites, a one-pot method

https://doi.org/10.1021/acs.analchem.5c06674
Anal. Chem. XXXX, XXX, XXX−XXX

Figure 3. continued

combining two optimization strategies with RPA was established to characterize the plasmid LOD for SARS-CoV-2 *N*, ALV-J *gp85*, and *Salmonella invA*. For B−M, NC represents the negative control without DNA substrate.

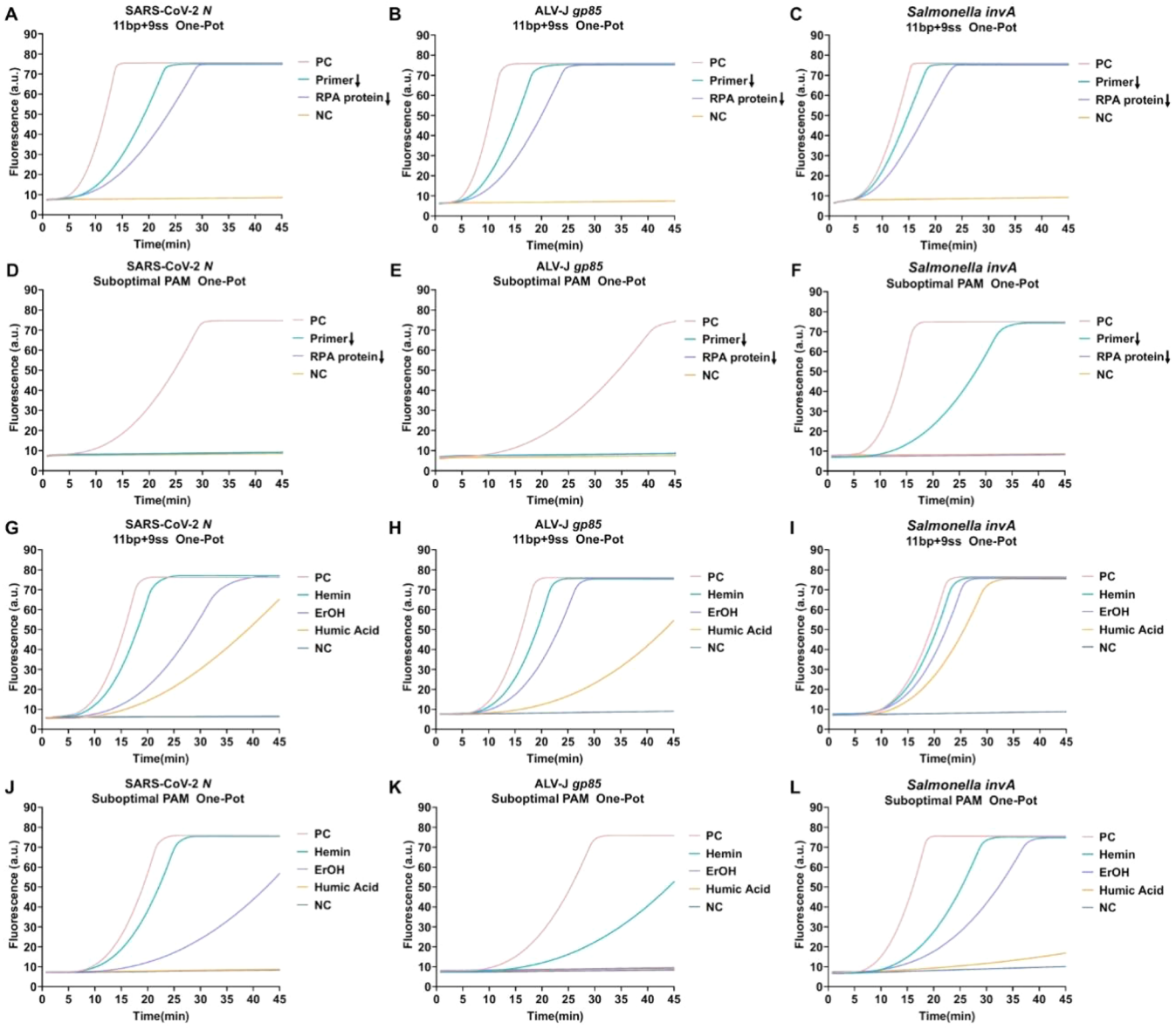


Figure 4. The robustness of the 11bp+9ss one-pot assay. (A, B, C) Based on the 11bp+9ss strategy, the detection performance of SARS-CoV-2 *N*, ALV-J *gp85*, and *Salmonella invA* was compared under a suboptimal RPA system using crRNAs targeting conventional sites. (D, E, F) Using a suboptimal PAM scheme, compare the detection performance of SARS-CoV-2 *N*, ALV-J *gp85*, and *Salmonella invA* under a suboptimal RPA system. For (A−F), PC represents the positive control, which is a one-pot reaction established by adding the conventional RPA system. The experimental groups involved reducing the RPA primers from 20 μM to 2 μM, and reducing the amount of RPA protein to half of the original. (G, H, I) Detection performance of SARS-CoV-2 *N*, ALV-J *gp85*, and *Salmonella invA* using the 11bp+9ss assay targeting canonical PAM, with or without environmental contaminants. (J, K, L) Detection performance of SARS-CoV-2 *N*, ALV-J *gp85*, and *Salmonella invA* using the suboptimal PAM-based assay, with or without environmental contaminants. For (A−L), the plasmid substrate concentration detected in each experiment was 1 × 10^6 copies/μL. NC represents the negative control without DNA substrate.

strong fluorescence signals for G496S while producing nearly no signal for G496, suggesting its potential for the specific diagnosis of Omicron BA.1 (Figure 2D−I).

Establishment of the 11bp+9ss One-Pot Assay

We subsequently integrated RPA with the 11bp+9ss strategy to establish a one-pot assay. To prevent potential false positives caused by extension of the ssDNA by the RPA polymerase, its 3′ end was modified with dideoxycytosine (ddC) (Figure 3A). Using plasmids as target substrates, the 11bp+9ss one-pot assay targeting canonical PAM sites in the SARS-CoV-2 *N*, ALV-J *gp85* and *Salmonella invA* genes achieved LOD of 1 × 10^0 copies/μL (Figure 3B,E,H). In contrast, the LOD achieved with assays targeting suboptimal PAMs were 1 × 10^2 copies/μL, 1 × 10^6 copies/μL, and 1 × 10^4 copies/μL for the three

https://doi.org/10.1021/acs.analchem.5c06674
Anal. Chem. XXXX, XXX, XXX−XXX

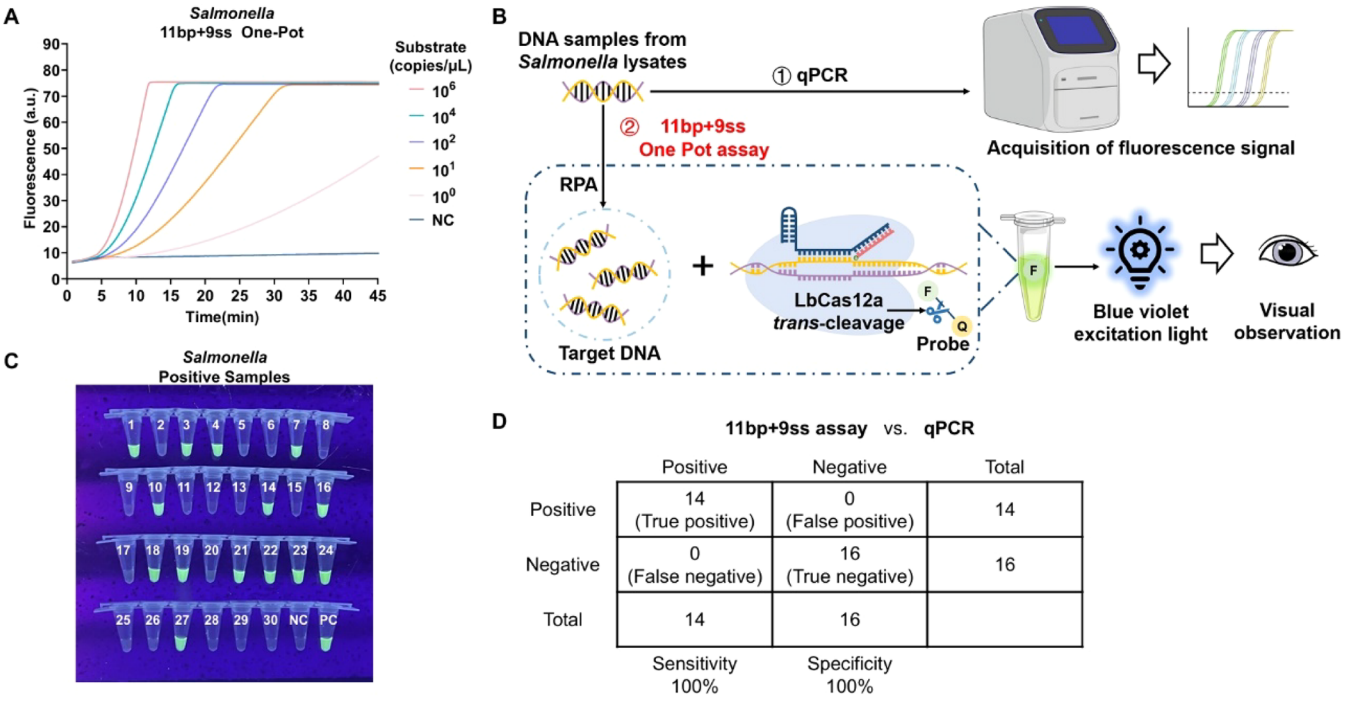


Figure 5. Detection of *Salmonella* using the 11bp+9ss one-pot assay. (A) After performing gradient dilutions of the lysed DNA samples of *Salmonella*, the LOD for the 11bp+9ss one-pot assay was assessed. (B) Schematic diagram illustrating the detection of *Salmonella* samples collected from newly laid eggshell surfaces using qPCR and the 11bp+9ss one-pot assay, respectively. (C) After incubation at 37 °C for 30 min, the fluorescence of positive samples detected by the 11bp+9ss one-pot assay can be directly visualized under blue light. PC represents positive samples, and NC represents negative samples. (D) Table showing the consistency between the 11bp+9ss one-pot assay and qPCR for 30 actual *Salmonella* samples.

targets, respectively (Figure 3C,F,I). By comparison, the one-pot assay employing canonical PAM targets yielded an LOD of 1×10^6 copies/μL or was nearly undetectable (Figure 3D,G,J). Based on these observations, we further optimized our strategy by combining suboptimal PAMs with the 11bp+9ss assay, which improved the LOD to 1×10^0 copies/μL (Figure 3K,L,M). Fluorescence values obtained using the 11bp+9ss assay were quantified by calculating their point of inflection (POI).[21] The regression curves for detection of the canonical ALV-J *gp85* target and the suboptimal SARS-CoV-2 *N* target using the 11bp+9ss assay yielded $R^2 < 0.9$ (Figure S6B,E), whereas all other targets showed $R^2 > 0.9$ (Figure S6A,C,F,G). These results indicate that although the 11bp+9ss one-pot assay did not achieve ideal quantitative performance, it exhibited high detection sensitivity overall.

Robustness of the 11bp+9ss One-Pot Assay under Suboptimal Conditions

RPA is a complex multiprotein system, and its amplification efficiency can be compromised in practice by various factors. To simulate such suboptimal RPA conditions, we independently reduced the concentrations of primers and RPA proteins. Detection results for the SARS-CoV-2 *N*, ALV-J *gp85*, and *Salmonella invA* genes demonstrated that the 11bp+9ss one-pot assay remained effective under suboptimal RPA amplification, exhibiting only a slight delay in detection time (Figure 4A,B,C). In contrast, one-pot assays based on suboptimal PAMs lost efficacy under the same suboptimal RPA conditions (Figure 4D,E,F). In practical detection, environmental contaminants may also interfere with assay performance. We evaluated the robustness of the 11bp+9ss one-pot assay in the presence of hemin (from plasma samples),[18] ethanol (EtOH, from nucleic acid extracts),[19] and humic acid (from soil or farm litter-contaminated fecal samples).[20] SARS-CoV-2 *N*, ALV-J *gp85*, and *Salmonella invA* were all successfully detected (Figure 4G,H,I). In contrast, these contaminants severely impaired the performance of assays targeting suboptimal PAM sequences; notably, humic acid abolished detection at all three target sites (Figure 4J,K,L). These results indicate that the proposed 11bp+9ss one-pot assay exhibits considerable robustness.

Detection of *Salmonella* Using 11bp+9ss One-Pot Assay

Salmonella is one of the most common foodborne pathogens found in eggs, meat, and meat products.[27,28] The International Commission on Microbiological Specifications for Foods, the European Union, and the Codex Alimentarius Commission require that *Salmonella* should not be detected in any of 60 samples collected from the same batch ($n = 60$, $c = 0$),[29] making detection assay with a consistent and low LOD crucial. The 11bp+9ss one-pot assay targeting the *Salmonella invA* gene was used to detect *Salmonella* in bacterial lysates, achieving an LOD of 1×10^0 copies/μL (Figure 5A). When the assay was tested against other bacterial species, signals were detected only for *Salmonella*, confirming its high specificity (Figure S7). Subsequently, the assay was applied to samples collected from egg surfaces. *Salmonella* detection was determined by visual assessment under blue light, and the results were compared with those obtained by qPCR (Figure 5B). The results showed 100% concordance between the 14 samples visually identified as positive under blue light and the positive results confirmed by qPCR (Figure 5C,D). These findings demonstrate the effectiveness of the 11bp+9ss one-pot assay for bacterial detection.

https://doi.org/10.1021/acs.analchem.5c06674
Anal. Chem. XXXX, XXX, XXX−XXX

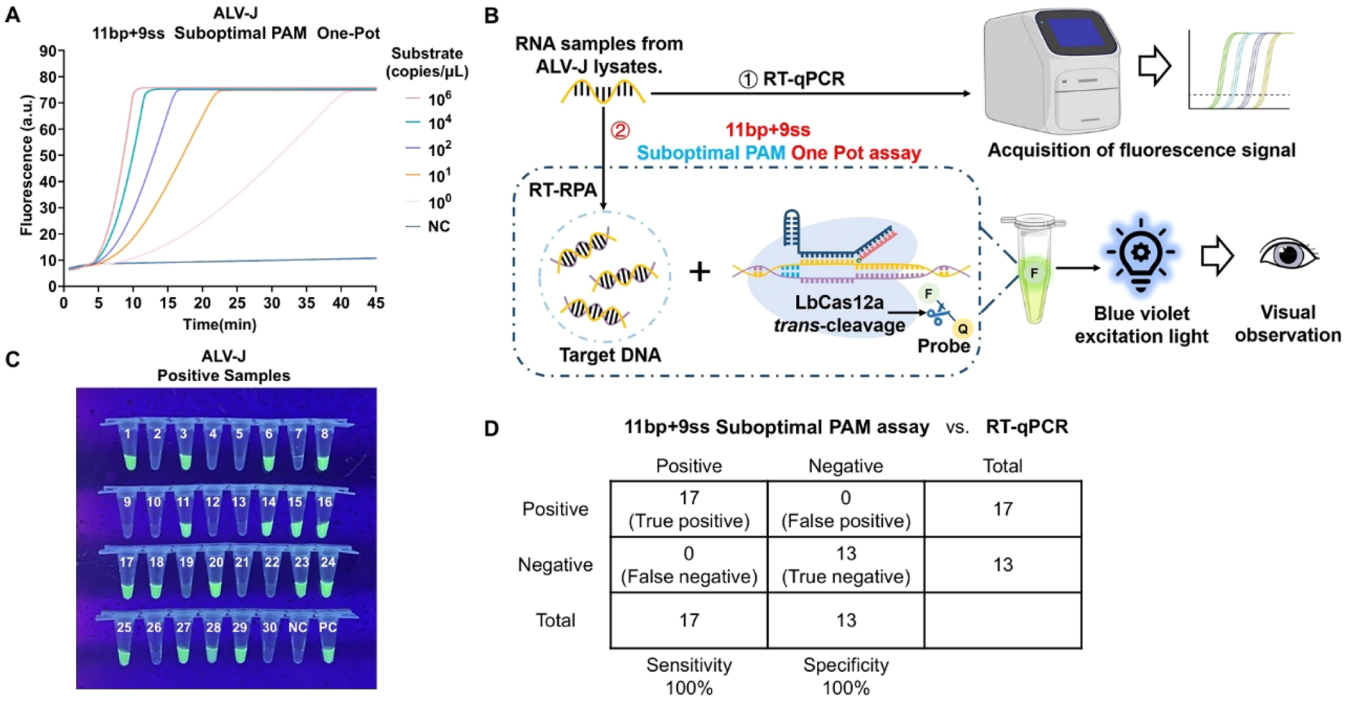


Figure 6. Detection of ALV-J using the one-pot method. (A) Gradually dilute the lysate samples of ALV-J and determine the LOD of this one-pot method. (B) A schematic diagram illustrating the detection of ALV-J in neonatal chicken meconium using RT-qPCR and the 11bp+9ss Suboptimal PAM one-pot assay, respectively. (C) After incubation at 37 °C for 30 min, the positive samples detected using the (11bp+9ss) + (Suboptimal PAM) one-pot assay exhibited fluorescence under blue light that could be directly visualized. PC represents positive samples, and NC represents negative samples. (D) Table showing the consistency between the (11bp+9ss) + (Suboptimal PAM) one-pot assay and RT-qPCR for 30 actual ALV-J samples.

Detection of ALV-J Using 11bp+9ss One-Pot Assay

Avian leukosis virus (ALV), belonging to the genus *Alpharetrovirus* within the family *Retroviridae*, is classified into 11 subgroups (A−K). Among these, subgroup J (ALV-J) is highly pathogenic and epidemic. As ALV-J is primarily transmitted vertically and no commercial vaccine is available, its control relies on eliminating infected chickens, creating a strong demand for POCT.[30,31] Given the substantial genetic diversity of ALV, we first analyzed the sequence conservation across multiple strains and identified a suboptimal PAM site with high universality, where 89% of the target sequences were completely conserved and 11% differed by only a single nucleotide (Figure S8). Viral particles of ALV-J were detected using the 11bp+9ss one-pot assay, which achieved an LOD of 1×10^0 copies/μL (Figure 6A). When the assay was applied to other viruses, signals were observed only for ALV-J, confirming its high specificity (Figure S9). The assay was subsequently used to test ALV-J in chick fecal samples, and the results were compared with those obtained by RT-qPCR (Figure 6B). The assay identified 17 positive samples under blue light, showing 100% concordance with the positive results confirmed by RT-qPCR (Figure 6C,D), demonstrating the applicability of this assay for virus detection.

DISCUSSION

This study maintained the double-stranded state of the dsDNA substrate by employing shortened complementarity to eliminate *cis*-cleavage. Previous research suggested that a minimum of 17 complementary base pairs were required for *cis*-cleavage, with the assumption that insufficient complementarity fails to activate the cleavage activity of Cas12a.[32] Our findings, however, indicate that for certain targets, as few as 11 base pairs can activate the RuvC domain (Figure 1), suggesting that in some contexts, it is the double-stranded state—rather than the lack of RuvC activation—that governs *cis*-cleavage. This conclusion is consistent with a recent study, which demonstrated that the *cis*- and *trans*-cleavage activities of Cas12a are functionally independent due to the relative positions of the nontemplate strands in proximity to RuvC domain.[15] This insight provides a new direction for optimizing Cas12a protein performance.

To enhance Cas12a activation, we employed an additional ssDNA molecule as a synergistic activator, constituting a dual-activator strategy utilizing both dsDNA and ssDNA. The dual-activator approach was initially reported using two ssDNA molecules, which was shown to improve the single-nucleotide discrimination capability of Cas12a on ssDNA targets.[24] Another study demonstrated that pre-addition of an RNA activator could modulate the activity, specificity, programmability, and sensitivity of Cas12a toward ssDNA and dsDNA targets.[33] Consistent with these findings, our study reveals that rational design of the ssDNA coactivator (e.g., by length shortening or introducing mismatches) allows flexible tuning of Cas12a activity and enables single-nucleotide specificity on dsDNA targets. The dual-activator strategy has been applied in other contexts: for instance, using dsDNA combined with RNA as activators enabled Cas12a-mediated RNA detection,[34] while a combination of ssDNA and dsDNA induced exon unwinding, thereby eliminating the PAM constraint for Cas12a.[35] Compared to strategies involving protein engineering[36] or crRNA modification,[37−39] the dual-activator approach

https://doi.org/10.1021/acs.analchem.5c06674
Anal. Chem. XXXX, XXX, XXX−XXX

offering advantages in flexibility, operational simplicity, and cost-effectiveness.

The most distinct feature of this study, compared to existing dual-activator research, lies in the length of the dsDNA activator. Since *cis*-cleavage activity removes the PAM-distal region of both dsDNA and ssDNA activators, it remains unaffected by substrate length, leaving the Cas12a catalytic domain fully exposed—which underlies its high *trans*-cleavage activity.[17] In our system, where Cas12a lacks *cis*-cleavage activity, the retained PAM-distal portion of the dsDNA may hinder the accessibility of the Cas12a catalytic site. This may explain the observed attenuation of *trans*-cleavage activity with longer DNA fragments across multiple targets. One potential solution to this limitation could be probe optimization. For instance, Cas9 was initially thought to lack *trans*-cleavage activity; however, after probe optimization, such activity was detected, presumably due to improved accessibility to the active site.[40] Notably, although the sensitivity of *trans*-cleavage activity to substrate length varied among targets in our study, substantial activity was retained for substrates shorter than 200 bp. Given that the optimal size of RPA amplicons is below 200 bp, the absence of *cis*-cleavage does not compromise the compatibility of our system with RPA. Interestingly, while previous studies indicated that Cas12a could not be activated by two ssDNA activators if the inner region of one exceeded 6 nt,[41] we observed no such constraint when using dsDNA as an activator. We speculate that these differences may stem from distinct spatial configurations adopted by dsDNA and ssDNA when bound to the Cas12a-crRNA complex. While the energy requirements for activating Cas12a cleavage by ssDNA, dsDNA, and RNA have been extensively studied, the differences in their spatial conformations represent a promising new area.

The one-pot assay integrates multiple reactions within a single system, typically involving RT, RPA, and CRISPR-based detection. Commercial systems already combine RT and RPA due to their relatively low interference. In contrast, RPA and CRISPR are inherently incompatible, as the former is an amplification reaction while the latter is a cleavage-based reaction. Current strategies to mitigate this conflict often involve attenuating CRISPR cleavage activity to favor RPA amplification.[13,14] However, given that RPA is a complex multiprotein system,[42,43] it cannot be guaranteed that RPA amplification will consistently outperform CRISPR cleavage under all conditions. By eliminating *cis*-cleavage, our study fundamentally resolves this incompatibility inherent in one-pot assays, thereby offering a particular advantage in suboptimal RPA amplification. An example is that pathogen lysis—which often involves reagents detrimental to protein activity—still requires a separate step and has not been successfully integrated into one-pot system. Based on our 11bp+9nt system, the feasibility of developing an integrated lysis−amplification−detection one-pot assay is significantly enhanced.

■ ASSOCIATED CONTENT

Supporting Information

The Supporting Information is available free of charge at https://pubs.acs.org/doi/10.1021/acs.analchem.5c06674.

Figures S1−S9: Supplementary validation of other genes; Tables S1−S12: All primer sequences (PDF)

■ AUTHOR INFORMATION

Corresponding Author

Xiaochuan Tang − *College of Animal Science and Technology, Guangxi University, Nanning, Guangxi 530004, China*; Email: tangxiaochuan7@163.com

Authors

Ruiying Han − *College of Animal Science and Technology, Guangxi University, Nanning, Guangxi 530004, China*; orcid.org/0009-0008-2383-3087

Ning Xiao − *Guangxi Academy of Sciences, Nanning, Guangxi 530007, China*

Zhirui Wu − *College of Animal Science and Technology, Guangxi University, Nanning, Guangxi 530004, China*

Yingying Zhao − *College of Animal Science and Technology, Guangxi University, Nanning, Guangxi 530004, China*

Xiaoli Wang − *College of Animal Science and Technology, Guangxi University, Nanning, Guangxi 530004, China*

Complete contact information is available at: https://pubs.acs.org/10.1021/acs.analchem.5c06674

Author Contributions

X.-C.T. designed the experiments. R.-Y.H. carried out the main experiments. R.-Y.H. performed the data analysis and wrote the manuscript. Other authors participated in some experiments. All authors discussed the results and commented on the manuscript.

Notes

The authors declare no competing financial interest.

■ ACKNOWLEDGMENTS

This work was supported by the Guangxi Natural Science Foundation Project (2025GXNSFAA069363, 2023GXNSFAA026260). The authors also thank all of the reviewers for their constructive comments.

■ REFERENCES

(1) Feng, W.; Newbigging, A.M.; Le, C.; Pang, B.; Peng, H.; Cao, Y.; Wu, J.; Abbas, G.; Song, J.; Wang, D.B.; et al. Molecular Diagnosis of COVID-19: Challenges and Research Needs. *Anal. Chem.* **2020**, *92* (15), 10196−10209.

(2) Broughton, J. P.; Deng, X.; Yu, G.; Fasching, C. L.; Servellita, V.; Singh, J.; Miao, X.; Streithorst, J. A.; Granados, A.; Sotomayor-Gonzalez, A.; et al. CRISPR−Cas12-based detection of SARS-CoV-2. *Nat. Biotechnol* **2020**, *38* (7), 870−874.

(3) Nouri, R.; Tang, Z.; Dong, M.; Liu, T.; Kshirsagar, A.; Guan, W. CRISPR-based detection of SARS-CoV-2: A review from sample to result. *Biosens. Bioelectron.* **2021**, *178*, 113012.

(4) Osório, N.S.; Correia-Neves, M. Implication of SARS-CoV-2 evolution in the sensitivity of RT-qPCR diagnostic assays. *Lancet Infect. Dis.* **2020**, *21* (2), 166−167.

(5) Vogels, C.B.; Brito, A.F.; Wyllie, A.L.; Fauver, J.R.; Ott, I.M.; Kalinich, C.C.; Petrone, M.E.; Casanovas-Massana, A.; Catherine Muenker, M.; Moore, A.J.; et al. Analytical sensitivity and efficiency comparisons of SARS-CoV-2 RT-qPCR primer-probe sets. *Nat. Microbiol* **2020**, *5* (10), 1299−1305.

(6) Chen, J. S.; Ma, E.; Harrington, L. B.; et al. CRISPR-Cas12a target binding unleashes indiscriminate single-stranded DNase activity. *Science* **2018**, *360* (6387), 436−439.

(7) Li, S.-Y.; Cheng, Q.-X.; Liu, J.-K.; Nie, X.-Q.; Zhao, G.-P.; Wang, J.; et al. CRISPR-Cas12a has both cis- and trans-cleavage activities on single-stranded DNA. *Cell Res.* **2018**, *28* (4), 491−493.

(8) Bravo, K. B. J.; Hallmark, T.; Naegle, B.; Beisel, C. L.; Jackson, R. N.; Taylor, D. W.; et al. RNA targeting unleashes indiscriminate nuclease activity of CRISPR−Cas12a2. *Nature* **2023**, *613* (7944), 582−587.
(9) Hu, M.; Liu, R.; Qiu, Z.; Cao, F.; Tian, T.; Lu, Y.; Jiang, Y.; Zhou, X.; et al. Light-start CRISPR-Cas12a reaction with caged crRNA enables rapid and sensitive nucleic acid detection. *Angew. Chem. Int. Ed.* **2023**, *62* (23), No. e202300663.
(10) Hu, F.; Liu, K.; Zhang, Y.; et al. Short-Time Preamplification-Assisted One-Pot CRISPR Nucleic Acid Detection Method with Portable Self-Heating Equipment for Point-of-Care Diagnosis. *Anal. Chem.* **2025**, *97*, 658−666.
(11) Hu, M.; Qiu, Z.; Bi, Z.; Tian, T.; Jiang, Y.; Zhou, X. Photocontrolled crRNA activation enables robust CRISPR-Cas12a diagnostics. *Proc. Natl. Acad. Sci. U. S. A.* **2022**, *119* (26), No. e2092933177.
(12) Chen, Y.; Xu, X.; Wang, J.; Zhang, Y.; Zeng, W.; Liu, Y.; Zhang, X Photoactivatable CRISPR/Cas12a Strategy for One-Pot DETECTR Molecular Diagnosis. *Anal. Chem* **2022**, *94* (27), 9724−9731.
(13) Lu, S.; Tong, X.; Han, Y.; Zhang, K.; Zhang, Y.; Chen, Q.; Duan, J.; Lei, X.; Huang, M.; Qiu, Y.; Zhang, D.-Y.; et al. Fast and sensitive detection of SARS-CoV-2 RNA using suboptimal protospacer adjacent motifs for Cas12a. *Nat. Biomed. Eng* **2022**, *6* (3), 286−297.
(14) Cheng, Z. H.; Luo, X. Y.; Yu, S. S.; Min, D.; Zhang, S. X.; Li, X. F.; Chen, J. J.; Liu, D. F.; Yu, H. Q.; et al. Tunable control of Cas12 activity promotes universal and fast one-pot nucleic acid detection. *Nat. Commun* **2025**, *16* (1), 1166.
(15) Huang, Z.; Song, Z.; Zeng, J.; Liu, X.; Fang, M.; Wu, Z.; Zhao, Y.; Chen, Y.; Li, D.; Huang, H.; Fu, L.; et al. Sensitive pathogen DNA detection by a multi-guide RNA Cas12a assay favoring trans- versus cis-cleavage. *Nat. Commun.* **2025**, *16* (1), 8257.
(16) Chao, L.; Shi-Yuan, L.; Jia-Kun, L.; et al. The CCTL (Cpf1-assisted Cutting and Taq DNA ligase-assisted Ligation) method for efficient editing of large DNA constructs in vitro. *Nucleic Acids Res.* **2017**, *45* (9), No. e74.
(17) Swarts, D. C.; Jinek, M. Mechanistic Insights into the cis- and trans-Acting DNase Activities of Cas12a. *Mol. Cell* **2019**, *73* (3), 589−600.e4.
(18) Sidstedt, M.; Hedman, J.; Romsos, E. L.; Waitara, L.; Wadsö, L.; Steffen, C. R.; Vallone, P. M.; Rådström, P. Inhibition mechanisms of hemoglobin, immunoglobulin G, and whole blood in digital and real-time PCR. *Anal. Bioanal. Chem* **2018**, *410* (10), 2569−2583.
(19) Kellner, M. J.; Koob, J. G.; Gootenberg, J. S.; Abudayyeh, O. O.; Zhang, F.; et al. SHERLOCK: nucleic acid detection with CRISPR nucleases. *Nat. Protoc.* **2019**, *14* (10), 2986−3012.
(20) Zheng, Y.; Liu, G.; Wu, Q.; Tan, M.; Xue, J.; Zhang, R.; Chen, D.; Xiao, Y.; Lv, M.; Liao, M.; Qu, S.; et al. Development of specific and rapid detection of human DNA by recombinase polymerase amplification assay for forensic analysis. *Forensic Sci. Int.: Genet* **2023**, *66*, 102903.
(21) Yao, Z.; He, K.; Wang, H.; Feng, S.; Ding, X.; Xu, Y.; Wang, Q.; Xu, X.; Wu, Q.; Wang, L. Tuning the Dynamic Reaction Balance of CRISPR/Cas12a and RPA in One Pot: A Key to Switch Nucleic Acid Quantification. *ACS Sens* **2024**, *9*, 3511−3519.
(22) Rambaut, A.; Holmes, E.C.; O'Toole, Á.; Hill, V.; McCrone, J.T.; Ruis, C.; Du Plessis, L.; Pybus, O.G. A dynamic nomenclature proposal for SARS-CoV-2 lineages to assist genomic epidemiology. *Nat. Microbiol* **2020**, *5* (11), 1403−1407.
(23) Dinah, P. Editorial: World Health Organization (WHO) Variants of Concern Lineages Under Monitoring (VOC-LUM) in Response to the Global Spread of Lineages and Sublineages of Omicron, or B.1.1.529, SARS-CoV-2. *Med. Sci. Monit* **2022**, *28*, No. e937676.
(24) Li, Q.; Song, Z.L.; Zhang, Y.; Zhu, L.; Yang, Q.; Liu, X.; Sun, X.; Chen, X.; Kong, R.; Fan, G.C Synergistic Incorporation of Two ssDNA Activators Enhances the Trans-Cleavage of CRISPR/Cas12a. *Anal. Chem* **2023**, *95* (23), 8879−8888.
(25) Xiao, H.; Hu, J.; Huang, C.; Feng, W.; Liu, Y.; Kumblathan, T.; Tao, J.; Xu, J.; Le, X. C.; Zhang, H.; et al. CRISPR techniques and potential for the detection and discrimination of SARS-CoV-2 variants of concern. *TrAC, Trends Anal. Chem.* **2023**, *161*, 117000.
(26) Sun, Q.; Lin, H.; Li, Y.; Yuan, L.; Li, B.; Ma, Y.; Wang, H.; Deng, X.; Chen, H.; Tang, S.; et al. A photocontrolled one-pot isothermal amplification and CRISPR-Cas12a assay for rapid detection of SARS-CoV-2 Omicron variants. *Microbiol. Spectrum* **2024**, *12*, No. e0364523.
(27) Barquist, L.; Langridge, G.C.; Turner, D.J.; Phan, M. D.; Turner, A.K.; Bateman, A.; Parkhill, J.; Wain, J.; Gardner, P.P. A comparison of dense transposon insertion libraries in the *Salmonella* serovars Typhi and Typhimurium. *Nucleic Acids Res.* **2013**, *41* (8), 4549−4564.
(28) Kirk, M. D.; Pires, S.M.; Black, R.E.; Caipo, M.; Crump, J.A.; Devleesschauwer, B.; Döpfer, D.; Fazil, A.; Fischer-Walker, C.L.; Hald, T.; et al. World Health Organization Estimates of the Global and Regional Disease Burden of 22 Foodborne Bacterial, Protozoal, and Viral Diseases, 2010: A Data Synthesis. *PLoS Med.* **2015**, *12* (12), No. e1001921.
(29) Liu, L.; Zhao, G.; Li, X.; Xu, Z.; Lei, H.; Shen, X. Development of rapid and easy detection of *Salmonella* in food matrics using RPA-CRISPR/Cas12a method. *LWT* **2022**, *162*, 113443.
(30) Pan, W.; Gao, Y.; Qin, L.; et al. Genetic diversity and phylogenetic analysis of glycoprotein GP85 of ALV-J isolates from China's mainland between 1999 and 2010: Coexistence of two extremely different subgroups in layers. *Vet. Microbiol* **2012**, *156* (1−2), 205−212.
(31) Li, Y.; Fu, J.; Cui, S.; Meng, F.; Cui, Z.; Fan, J.; Chang, S.; Zhao, P. Gp85 genetic diversity of avian leukosis virus subgroup J. among different individual chickens from a native flock. *Poult. Sci.* **2017**, *96* (5), 1100−1107.
(32) Kleinstiver, B.P.; Tsai, S.Q.; Prew, M.S.; Nguyen, N.T.; Welch, M.M.; Lopez, J.M.; McCaw, Z.R.; Aryee, M.J.; Joung, J.K. Genome-wide specificities of CRISPR-Cas Cpf1 nucleases in human cells. *Nat. Biotechnol* **2016**, *34* (8), 869−874.
(33) Zhao, R.; Luo, W.; Wu, Y.; Zhang, L.; Liu, X.; Li, J.; Yang, Y.; Wang, L.; Wang, L.; Han, X.; et al. Unmodificated stepless regulation of CRISPR/Cas12a multi-performance. *Nucleic Acids Res.* **2023**, *51* (19), 10795−10807.
(34) Rananaware, S.R.; Vesco, E.K.; Shoemaker, G.M.; Anekar, S.S.; Sandoval, L.S.W.; Meister, K.S.; Macaluso, N.C.; Nguyen, L.T.; Jain, P.K. Programmable RNA detection with CRISPR-Cas12a. *Nat. Commun.* **2023**, *14* (1), 5409.
(35) Huang, S.; Lou, Y.; Zheng, L. Synergistic effect of split DNA activators of Cas12a with exon-unwinding and induced targeting effect. *Nucleic Acids Res.* **2024**, *52*, 11148−11157.
(36) Aman, R.; Mahas, A.; Mahfouz, M. Nucleic Acid Detection Using CRISPR/Cas Biosensing Technologies. *ACS Synth. Biol.* **2020**, *9* (6), 1226−1233.
(37) Chen, Y.; Wang, X.; Zhang, J.; Jiang, Q.; Qiao, B.; He, B.; Yin, W.; Qiao, J.; Liu, Y.; et al. Split crRNA with CRISPR-Cas12a enabling highly sensitive and multiplexed detection of RNA and DNA. *Nat. Commun.* **2024**, *15* (1), 8342.
(38) Liu, Y.; Liu, X.; Wei, D.; Dang, L.; Xu, X.; Huang, S.; Li, L.; Wu, S.; Wu, J.; Liu, X.; et al. CoHIT: a one-pot ultrasensitive ERA-CRISPR system for detecting multiple same-site indels. *Nat. Commun.* **2024**, *15* (1), 5014.
(39) Zhang, J.; Yin, W.; Jiang, Q.; Mao, W.; Deng, W.; Jin, S.; Wang, X.; He, R.; Qiao, J.; Liu, Y.; et al. Precise amplification-free detection of highly structured RNA with an enhanced SCas12a assay. *Commun. Biol* **2025**, *8* (1), 366.
(40) Chen, J.; Chen, Y.; Huang, L.; Lin, X.; Chen, H.; Xiang, W.; Liu, L. Trans-nuclease activity of Cas9 activated by DNA or RNA target binding. *Nat. Biotechnol* **2024**, *43* (4), 558−568.
(41) Hu, M.; Cheng, X.; Wu, T. Modular CRISPR/Cas12a synergistic activation platform for detection and logic operations. *Nucleic Acids Res.* **2024**, *52*, 7384−7396.

https://doi.org/10.1021/acs.analchem.5c06674
Anal. Chem. XXXX, XXX, XXX−XXX

(42) Sun, Y.; Yu, L.; Liu, C.; Ye, S.; Chen, W.; Li, D.; Huang, W.; et al. One-tube SARS-CoV-2 detection platform based on RT-RPA and CRISPR/Cas12a. *J. Transl. Med.* **2021**, *19* (1), 74.
(43) Li, L.; Duan, J.-J.; Wei, X.-Y.; Hu, H.; Wang, Y.-B.; Jia, P.-P.; Pei, D.-S.; et al. Generation and application of a novel high-throughput detection based on RPA-CRISPR technique to sensitively monitor pathogenic microorganisms in the environment. *Sci. Total Environ* **2022**, *838* (2), 156048.



https://doi.org/10.1021/acs.analchem.5c06674
Anal. Chem. XXXX, XXX, XXX−XXX